J Mater Sci: Mater Med (2008) 19:2377–2387
DOI 10.1007/s10856-007-3276-2

Effects of carbon nanotubes (CNTs) on the processing and in-vitro degradation of poly(DL-lactide-*co*-glycolide)/CNT films

Ilaria Armentano · Mariaserena Dottori · Debora Puglia · Josè M. Kenny

Received: 22 January 2007 / Accepted: 7 September 2007 / Published online: 25 December 2007

Abstract Nanocomposite films based on single wall carbon nanotubes (SWNTs) and poly(DL-lactide-*co*-glycolide) copolymer (50:50 PLGA) were processed and analyzed. The purpose of this study was to investigate the effect of different functionalization systems on the physical stability and morphology of PLGA films. Both covalent and non covalent functionalization of carbon nanotubes were considered in order to control the interactions between PLGA and SWNTs and to understand the role of the filler in the biodegradation properties. Using a solvent casting process, different PLGA/SWNT nanocomposites were prepared and incubated using organic solution under physiological conditions. In-vitro degradation studies were conducted by measurements of weight loss, infrared spectroscopy, glass transition temperature and SEM observations as a function of the incubation time, over a 9-week period. All PLGA films were degraded by hydrolitical degradation. However, a different degradation mechanism was observed in the case of functionalized SWNTs with respect to pristine material. It has been observed that system composition and SWNT functionalization may play a crucial role on the autocatalytic effect of the degradation process. These studies suggest that the degradation kinetics of the films can be engineered by varying carbon nanotube (CNT) content and functionalization. The combination of biodegradable polymers and CNTs opens a new perspective in the self-assembly of nanomaterials and nanodevices.

I. Armentano (✉) · M. Dottori · D. Puglia · J. M. Kenny
Materials Engineering Centre, UdR INSTM, NIPLAB,
University of Perugia, Terni, Italy
e-mail: Ilaria.Armentano@lnl.infn.it

1 Introduction

Carbon structures have been the subject of extensive research [1] since the discovery of fullerenes and carbon nanotubes (CNTs) because of their exceptional mechanical and electrical properties, which are related to their unique structure and which makes them attractive for the development of innovative devices in several applied fields, including composites, sensors and nanoscale electronic devices [2–5]. Furthermore, there has been a tremendous interest in using the properties of CNTs to promising biological applications [6, 7]. There have been several recent investigations concerning the use of carbon nanotubes for biological purposes and their introduction in biological systems taking advantage of the fact that all living entities are carbon based and nanotubes are solely made of carbon with a similar scale size of DNA [8]. In recent years, there has been a significant interest in biological applications of novel solid-state nanomaterials. CNTs could be ideal in designing promising new tissue engineered products in biological applications and promising possibilities can be expected by introducing them to reinforce scaffolds for tissue engineering. CNTs, in fact, are one of the most promising candidates for the design of novel polymer composites [9, 10]. However, still scarce attention have been dedicated to analyze the eventual interactions of carbon tubes with living entities [6–8] and any future biomedical application should also consider these aspects.

Considerable efforts have been made to fabricate different carbon based molecular structures and to explore new applications in different fields including, among others, nanocomposites. The physical properties and performance of polymer matrix nanocomposites can be in fact significantly improved by the addition of small percentages of carbon nanotubes of less than 1% wt [9–11]. The main problem for these applications is the dispersion of the nanotubes and the creation of a good interface between the nanotubes and the polymer matrix. The role of the interface between the nanotubes and polymer matrix is essential in transferring the load from the matrix to the nanotubes, thereby enhancing the mechanical and electrical properties of the composite. The main objective in the development of nanocomposites is to transfer the unique properties of SWNTs to matrix materials increasing their added value [10, 11].

In our research, different techniques were explored to improve the CNT dispersion in a biopolymer matrix and improve the bioactivity of the composite. Both covalent and non covalent functionalization of the nanotube surface were considered in order to control the interactions between PLGA and SWNTs and to understand the role of the fillers in the biodegradation properties. The advantage of a non-covalent attachment is that the perfect structure of the SWNTs is not damaged and their properties remain intact. The disadvantage is that the forces between the polymer and the SWNT are very weak, which means that the load may not be transferred efficiently from the polymer matrix to the nanotube. Covalent functionalization could include fluorine, radicals, amine groups, etc, but the group that is most frequently attached to the CNT's sidewall are the carboxylic acid groups [12–14].

Polymers are applied in numerous biomedical applications and increasing attention has been paid to composites made of polymers and nanofillers for applications in tissue engineering. The combination of such polymers with CNTs takes advantage by controlling the matrix properties and the effect on polymer matrices. The composite is expected to have superior mechanical properties to the neat polymer matrix improving its structural integrity [9–11]. Good interfacial adhesion between the CNT and the polymer matrix is essential for efficient load transfer in the composite.

Degradation properties are of crucial importance in biomaterial selection and design [15–18]. The rate of degradation may affect a range of processes, such as cell growth, tissue regeneration, drug release and host response. In-vitro applications allow us to identify the bio-erosion mechanisms of the material mainly determined by the hydrolysis of the polymer matrix. Extensive literature on biodegradation of polymer materials reveals the complexity of the hydrolysis mechanism; it is important to understand not only the time the material employs to bio-erode itself but also in what conditions it will happen, in relation to the chemical composition of the samples, the pH of the medium, temperature, surface treatments, sample size and shape, reinforcing particles and particle functionalization [18–23].

In this study, PLGA/SWNT nanocomposite samples were analyzed at various degradation stages in order to elucidate the effects of SWNT introduction and functionalization on their hydrolytic degradation. So, the purpose of this paper is to present a report on the preparation of PLGA/SWNT nanocomposites and to investigate the in-vitro degradation of poly(DL-lactic-*co*-glycolic acid) (PLGA) films, combined with two different SWNTs, that is, pristine (PLGA/SWNT) and carboxylate (PLGA/SWNT-COOH) SWNTs.

2 Materials and methods

2.1 Materials

Poly(DL-lactide-*co*-glicolide) (PLGA) (inherent viscosity 0.58dl/g), a copolymer with a 50/50 ratio (PLA/PGA), was purchased from Absorbable Polymers-Lactel. Single wall nanotubes (SWNTs) were obtained from Thomas Swan. SWNTs with carboxyl groups (SWNTs-COOH) were purchased from Sigma Aldrich. This material contains a carboxylic acid functionality along the length of the nanotube which can be derivatized with a variety of functional groups. A commercially available grade of chloroform, supplied by Sigma-Aldrich Chemicals, was used in the nanocomposite preparation. Hepes and a NaOH deionized water solution were used as the in-vitro degradation medium. Solution concentration was 1 M and the pH was 7.0. All samples were analyzed after drying for 24 h at 37 °C.

2.2 Sample preparation

Nanocomposite films were prepared using a solvent casting technique. The solvent used was chloroform and the percentage of pristine and carboxylate SWNTs tested was 1% wt with respect to the matrix. CNTs (10 mg) were sonicated in chloroform to disperse the tubes. Thereafter, the polymer (1000 mg) was added and the suspension was sonicated until the entire polymer dissolved. The dispersion was cast in a substrate to remove all the solvent, leaving a nanocomposite film (approx. 300 μm). Samples were air dried for 48 h and to ensure the full evaporation of the solvent, each PLGA/SWNT composite sample was vacuum-dried for 24 h at room temperature.

2.3 In-vitro degradation studies

The degradation of the PLGA and PLGA/SWNT films was investigated in Hepes and NaOH solutions, under physiological conditions (pH 7.0 and 37 °C). The initial pre-weighed samples of the different formulations (PLGA, PLGA/SWNTs and PLGA/SWNTs-COOH) were placed in holders that contained 20 ml of the organic solution in each. The samples were stored in a 37 °C environment for long time periods.

Sample weight loss, morphological, compositional and thermal changes were systematically analyzed over a 4-week period of degradation in an organic solution at 37 °C. Some measurements were performed after up to 9 weeks of degradation.

2.4 Sample characterization

2.4.1 *Field Emission Scanning Electron Microscopy (FESEM)*

Field emission scanning electron microscopy was used to examine the morphology of the pristine and carboxylated SWNTs and the surface and the internal morphologies of the nanocomposite films before and after in-vitro degradation. Samples were characterized using a Supra 25 Zeiss FESEM.

SWNTs samples for SEM observation were prepared by dispersing the tubes in N,N-dimethylformamide (DMF), and immersing them in an ultrasonic bath for 30 min; few drops of the resulting suspension were placed onto silicon substrate and vacuum dried for 2 h.

2.4.2 *Thermal analysis (DSC-TGA)*

Thermal properties were characterized by a differential scanning calorimetry (DSC) Mettler Toledo 822e Model. Ten milligrams of dried samples were placed in covered aluminium sample pans and then placed in the DSC sample holder. The samples were then heated at 2 °C/min, in the -25 to 80 °C temperature range and in a nitrogen atmosphere. The values of the transition temperatures were obtained from the dynamic thermograms, using the midpoint between the intersections of the two parallel baselines, before and after the Tg. For the calculation of the glass transition temperature from dynamic scans, an average of three measurements was made for each sample.

Thermogravimetric analysis (TGA) was performed on 10 mg samples on a Seiko Exstar 6000 TGA quartz rod microbalance. The SWNTs and the nanocomposite films were investigated. The tests were done in air flow (50 ml*min^{-1}) from 30 to 900 °C with a 5 °C /min heating ramp in the case of CNTs and with a 10 °C /min for the nanocomposite films.

2.4.3 *Thermo-Dynamical Mechanical Analysis (TMA-DMA)*

The thermal expansion coefficient of the films was determined using a thermo-mechanical analyzer (TMA 7, PerkinElmer) from -2 to 60 °C at a heating rate of 2 °C /min and static force of 10 mN.

Dynamic-Mechanical Analysis (DMA) was performed by using a Reometric Scientific-ARES N_2. The sample size was 10 mm in width, 30 mm in length, and 0.3 mm in thickness. The measurements were made in the dynamic time sweep test at room temperature and frequency fixed at 1 Hz and shear strain at 0.3%. The storage modulus of the PLGA, PLGA/SWNTs and PLGA/SWNT-COOH samples was measured.

2.4.4 *Weight loss*

Samples of neat polymer and nanocomposites with dimensions of 3 mm × 3 mm and weighing approx. 10 mg (M_0) were cut for the degradation experiments. At each time point, 4 samples of each formulation were removed from the buffer and weighed (M) after drying for one day. The mass was measured to an accuracy of 0.01 mg using a Sartorius precision balance. Four samples of each composition were measured and the results averaged. All measurements were expressed as an average ± the standard deviation.

2.4.5 *Infrared spectroscopy*

Fourier infrared (FT-IR) spectra of the samples in the 400–4000-cm^{-1} range, operating in a transmission mode, were recorded using a Jasco FT-IR 615 spectrometer. Nanocomposite films were deposited by drop casting on silicon substrates and different spectra were recorded for any incubation time.

2.4.6 *pH changes*

The pH level of the surrounding medium was measured using an Orion 420A pH Meter. The measurement was always done on a volume of solution equal to 20 ml with an initial pH 7.0.

3 Results and discussion

3.1 SWNTs characterization

Figure 1 shows SWNT and SWNT-COOH SEM images. Noticeable amounts of SWNT bundles with a 50 nm

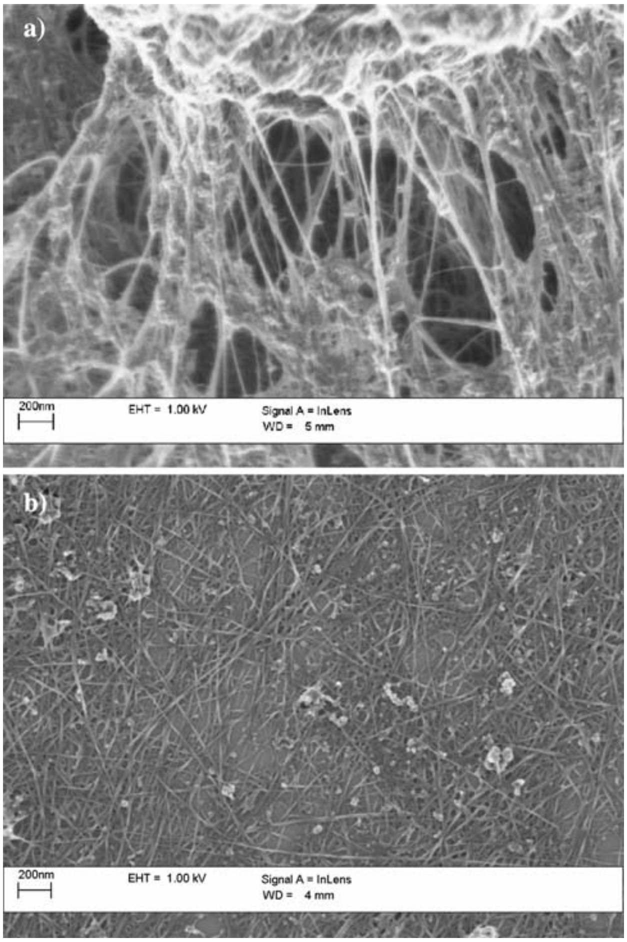

Fig. 1 FESEM micrographs of SWNTs (**a**) and SWNTs-COOH (**b**) on silicon substrates after dispersion in DMF, showing the layered structure of single walled carbon nanotube bundles

diameter were found in both materials, showing uniform diameter distribution.

Moreover, the thermal degradation of SWNT and SWNT-COOH samples in an oxidative atmosphere was monitored with a TGA, as reported in Fig. 2, with the purpose to analyze the purity of the nanotube samples used [11]. The percentage weight loss curve indicates that the overall weight loss during the process was nearly total for pristine and carboxylate SWNTs and the time derivative weight loss curve shows that only one main weight loss step characterizes the SWNTs degradation while two peaks are associated to SWNT-COOH tubes. Moreover, lower degradation temperatures were measured for carboxylate tubes. The lower thermal stability and the double degradation peak of carboxylate tubes is clearly attributed to the differential degradation of the attached functional groups and of the main tube structure. In both cases, a residual mass of about 4% weight at 800 °C is normally attributed to metal particles present as catalytic material during the synthesis. From the TGA thermograms it can be concluded that the purity of both nanotubes used in this research is higher than 95%.

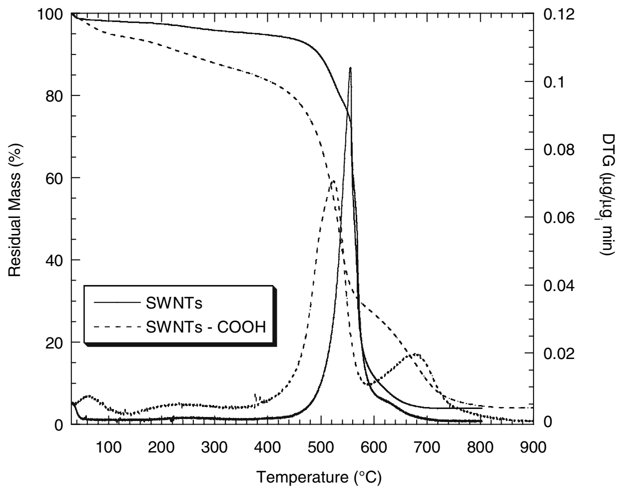

Fig. 2 TG and derivative oxidation thermograms of pristine SWNTs and SWNTs-COOH

3.2 Nanocomposite characterization

The fine structure of the PLGA/ SWNT films, on surface and transverse sections, was investigated at a high magnification. Figure 3 shows FESEM images of PLGA-SWNTs and PLGA-SWNTs-COOH on silicon substrates at different magnification. A large amount of SWNT bundles immersed in a polymer matrix are visible. Cross-sectioned samples were prepared in order to view the internal structure. It is interesting to note that this sample with SWNTs of 1% in weight, did not need to be sputter coated before taking images with the SEM; even with a small amount of SWNTs, it was conductive on its own [24]. The fine structure of the SWNTs-COOH in the PLGA is evident. Carboxylate tube bundles appeared with a better degree of matrix dispersion (Fig. 3b). In this case the long SWNTs-COOH were fragmented by means of chemical oxidation, which produced –COOH groups at the open end of the tubes [25].

Thermal characterization was performed on pure copolymer and on the nanocomposites. DSC measurements reveal that materials have an amorphous behaviour, with a glass transition of around 45 °C for all compositions. Differences were found analyzing thermomechanical properties. Figure 4a shows the TMA thermograms from -2 to 60 °C of the three materials. The thermal expansion coefficient of the nanocomposites decreases with the CNTs introduction. The thermal expansion of the copolymer films relating to the rubbery-like state, was found to be 110×10^{-3} °C^{-1} that decreases to 80×10^{-3} °C^{-1}

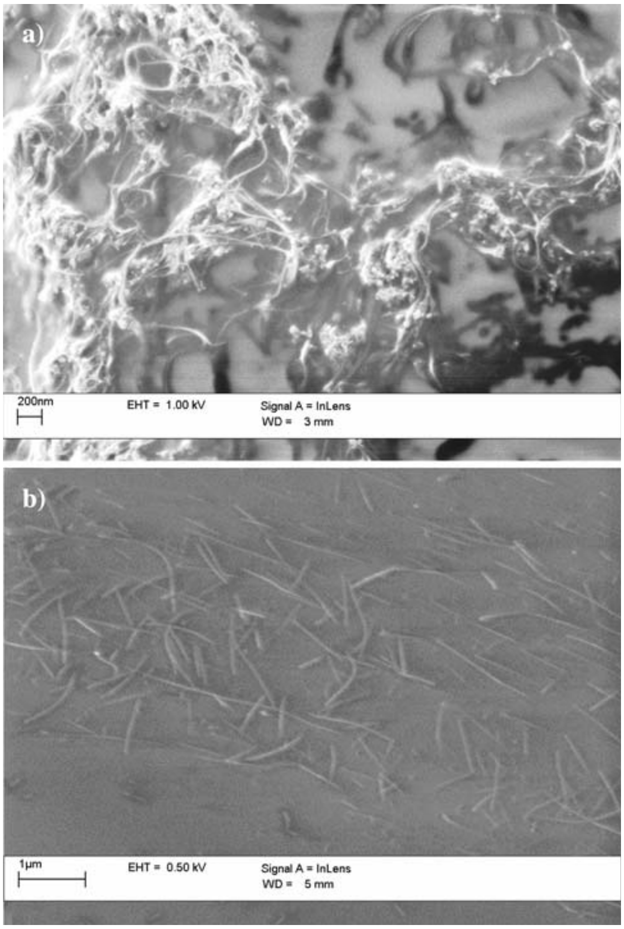

Fig. 3 The fine structure of the SWNTs-PLGA (**a**) and SWNT-COOH PLGA (**b**) at high magnification

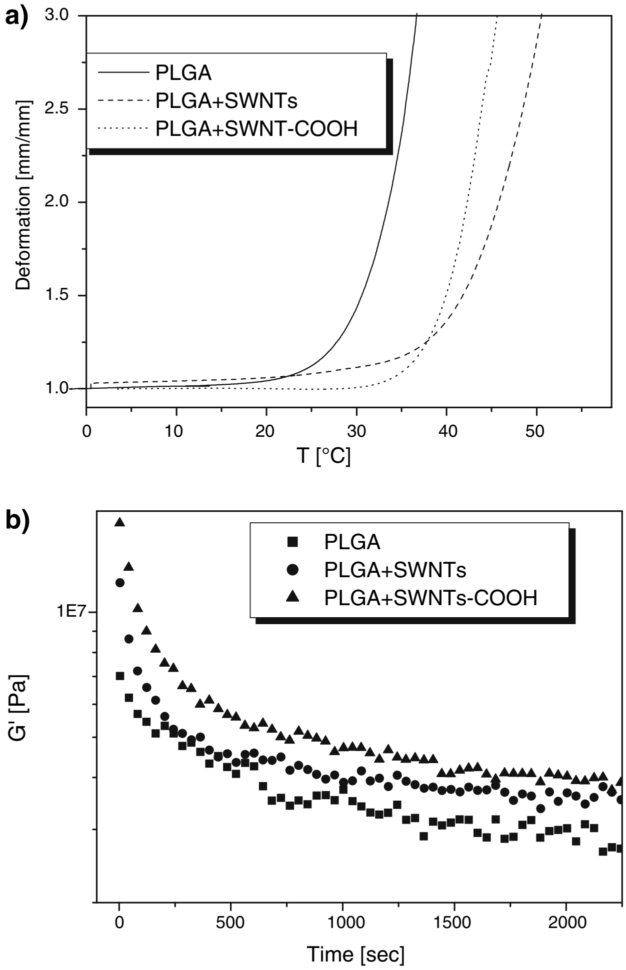

Fig. 4 TMA thermograms of pure PLGA and nanocomposite films (**a**). Dynamic time sweep of PLGA, PLGA-SWNTs and PLGA-SWNT-COOH nanocomposites (**b**)

introducing 1% weight percentage of carboxylate tubes and the lowest value was found with pristine SWNTs, obtaining 50×10^{-3} °C^{-1}. This suggested that the miscibility of PLGA and carboxylated nanotubes was higher than that of pristine nanotubes and dimensional stability of PLGA nanocomposite was increased by the presence of CNTs.

At least two parameters have to be taken into consideration in analysing the results, i.e. the presence of SWNTs incorporated in the polymer and the functionalization used to improve their adhesion to the matrix. To fully evaluate the effects of CNTs introduction and the role of functionalization treatment, dynamical mechanical analysis was performed on PLGA and nanocomposite based on CNTs. The storage modulus for the three materials was shown in Fig. 4b. PLGA is clearly a viscoelastic material, very sensitive to all few environmental changes. The storage modulus is quite slow, if compared to other biodegradable polymers. It is noticeable the reinforcing effect of carbon nanotubes. As seen in Fig. 4b, the storage modulus increases in the presence of CNTs in the nanocomposite, i.e., the storage modulus of SWNT-COOH based composites is higher than that of the unfilled PLGA matrix, which indicates that stress transfers from the matrix to the functionalized CNTs. Assuming Poisson Ratio of biodegradable polymer as 0.3 [26], the Young elastic modulus can be calculated from the following expression: $E_{YOUNG} = 2(1 + 2\nu)G' = 2.3G'$. All values were chosen at t = 2500s and the Young modulus of matrix was 5.0 MPa, that increases to 7.8 MPa when 1 %wt was introduced, but the higher value was found in the case of carboxylated tubes, the obtained value was 8.3 MPa.

Therefore, both DMA and TMA results suggest that nanocomposite based on SWNT-COOH should be more homogeneous than nanocomposite based on pristine tubes, the interface interaction was encouraged by carboxylic functionality.

3.3 Degradation studies

3.3.1 *Changes in thermal properties*

The changes of the Tg of the neat copolymer and of the two nanocomposites based on SWNTs and carboxylate nanotubes as a function of the degradation are shown in Fig. 5. Upon degradation, the Tg of the PLGA and PLGA/CNTs significantly decreases with the incubation time during the first part of the degradation process. This behaviour can be clearly associated to the plastification effect of water diffusing in the polymeric matrix upon exposure of the samples to the aqueous hydrolytic medium. At long degradation time a clear difference in the plastification behaviour as a function of the tube functionalization can be observed. Whilst in the case of the carboxylate tubes, the Tg values always decreases, for the other two materials, PLGA and PLGA/SWNTs, an increase in the Tg values after the first week is observed. The hardening effects of the hydrolytic degradation was also evident on a simple visual and tactile inspection of the samples and can be associated to a crosslinking of the polymer after partial chain scission by hydrolysis [28].

In all cases, pure matrix and nanocomposites, the hydrolytic degradation of the PLGA matrix is clearly controlled by two main mechanisms: chain-scission (decreasing the Tg, mainly evident in the initial stage) and cross-linking (increasing the Tg, typically evident at longer times).

3.3.2 *Weight loss*

Figure 6 displays the weight loss of the degrading PLGA, PLGA/SWNT and PLGA/SWNT-COOH films as a function of the incubation time in the biological fluid. The dynamics of weight loss for all the nanocomposites are similar to the neat PLGA behaviour in the first part of the hydrolytic degradation process. Initially, for all the materials studied, there is a gradual and slight reduction of the sample weight that continues for several days. After two weeks, a dramatic decrease in mass is observed in agreement with previous studies on other PLGA based composites [19, 27]. In the case of the carboxylate tubes, it was impossible to perform measurements after 18 days of incubation, as the sample was disaggregated in the solution and an increase in the degradation rate was evident. The PLGA/SWNT film samples exhibited a similar weight loss behaviour than the neat PLGA with destruction after 24 days. The faster mass loss in SWNT-COOH composites suggest a higher interaction of the functionalized tubes with the polymer matrix and the solvent leading to a more rapid erosion of the nanocomposite.

3.3.3 *Infrared spectroscopy*

The changes in the chemical composition of the polyester polymer and its nanocomposites, before and after incubation, were explored using FTIR. Indeed, upon simple visual inspection it was clear the degradation was not uniform through the surface of the films prepared for FTIR. So, IR spectra were recorded in different zones of the samples, but it is clear that no quantitative analysis of the hydrolytic degradation can be performed through FTIR. IR spectra of PLGA copolymer and PLGA/SWNT and PLGA/SWNT-COOH nanocomposites were recorded and are shown in Fig. 7. Spectra were registered on the same sample at different incubation times. IR studies were carried out in

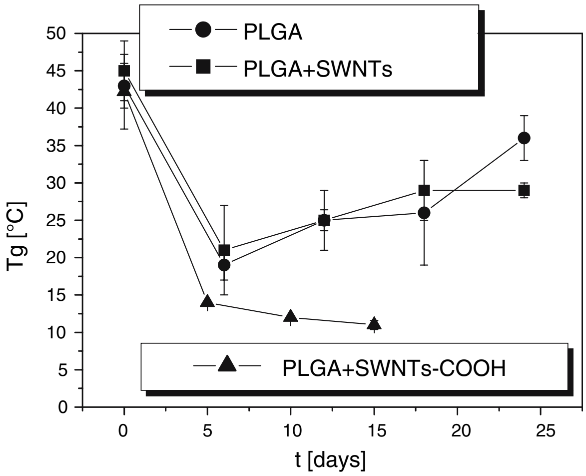

Fig. 5 Glass transition temperature (Tg) of PLGA, PLGA/SWNTs and PLGA/SWNTs-COOH as a function of degradation time

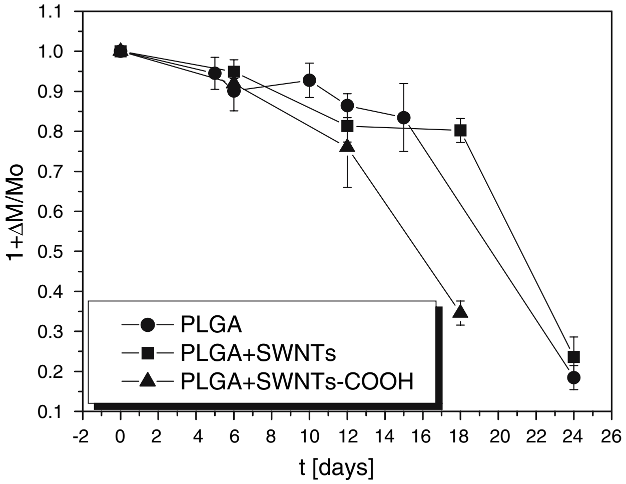

Fig. 6 Weight loss of degrading PLGA, PLGA/SWNTs and PLGA/SWNTs-COOH films as a function of incubation time

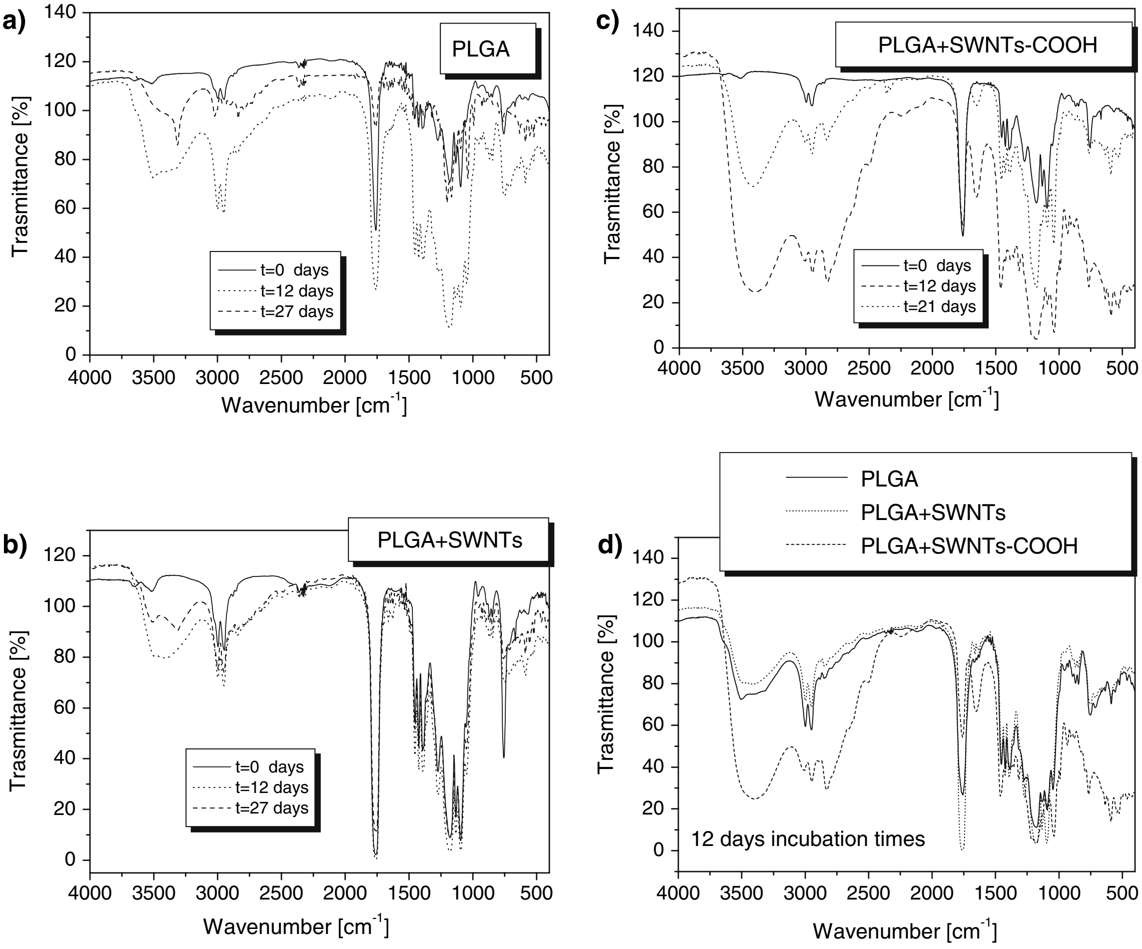

Fig. 7 FT-IR spectrum of PLGA (**a**), PLGA/SWNTs (**b**) PLGA/SWNTs-COOH (**c**) samples for different incubation times. FT-IR spectra of PLGA, PLGA/SWNTs and PLGA/SWNTs-COOH at 12 days incubation times (**d**)

four different regions. As previously reported [29–31] the first one refers to the aliphatic C–H stretching vibrations between 3000 and 2850 cm^{-1}, the second and third regions include the C=O stretching bands at 1850–1650 cm^{-1} and the asymmetric C–O stretching vibrations at 1300–1000 cm^{-1}, respectively; the fourth is the OH stretching region at 3700–3400 cm^{-1}. The absorbance of the aliphatic C–H stretching bands at around 2997, 2950 and 2883 cm^{-1} decreased for all the samples during the degradation period. However, a non-uniform decrease in different peaks can be observed, indicating a selective degradation of the sample.

The copolymers had characteristic C–O peaks at 1270, 1180, 1130, 1097 and 1044 cm^{-1}. Upon exposure to the degradation medium, not only the intensity of these absorption bands is reduced, but some of them are shifted and new bands in the region 1300–1000 cm^{-1} are formed.

The spectral evaluation was also performed in the region of the characteristic carbonyl stretching vibrations between 1850 and 1650 cm^{-1}. The specific interaction showed a decrease in the absorption frequency of the carbonyl group (C=O) and an increase in the OH stretching showing a large band at 3400 cm^{-1} [32–34]. For the CNTs-PLGA nanocomposites, before degradation, similar spectra are obtained as the concentration of CNTs is too small to produce changes in the PLGA spectra. Figure 7d shows the spectra of the three different materials after 12 days of incubation. Upon degradation similar qualitative conclusions with respect to those from weight loss can be obtained. In fact, SWNT composites show a similar behaviour than neat PLGA after 12 days of hydrolytic degradation, while functionalized SWNT-COOH nanocomposites offered a different spectra indicating a quicker degradation mechanism.

3.3.4 *Morphological changes*

The gross appearance of all the PLGA films changed over time during degradation. The amorphous PLGA film samples were initially almost transparent. As degradation proceeded, they became whitish due to water absorption. Then they became brittle and began to disintegrate in agreement with previous publications [17]. The visual aspects of PLGA and PLGA/SWNT films during degradation seem to be different; the typical swelling of the hydrophilic PLGA is inhibited by the presence of the SWNTs in the nanocomposite, confirming the TMA data on the decreasing of thermal expansion coefficient in the nanocomposite films.

The changes in surface morphology caused by hydrolysis, were observed using a Field Emission Scanning Electron Microscopy (FESEM). Figure 8 shows the morphology of nanocomposites containing SWNTs after 4 weeks (a) and 9 weeks of incubation (b). After 4 weeks in-vitro, the nanocomposite films developed large pores on the surface due to polymer degradation. After 9 weeks of extensive degradation, the samples became more and more irregular leading to eventual fragmentation and SWNT bundles became visible on the surface. It is evident in Fig. 8b the increasing porosity of the nanocomposites as the hydrolytic degradation of the polymer matrix progresses revealing a higher number of CNTs on the surface. The situation in the case of carboxylate tubes was different. Comparative FESEM images of PLGA/SWNTs and PLGA/SWNT-COOH with the same magnification and at the same degradation time (9 weeks) were also shown in Fig. 8. Whilst samples based on SWNTs revealed large amounts of microporous systems, indicating a localized selective degradation, in the case of the carboxylate tubes, the degraded surface appears uniform. In Fig. 9, the two different medium are shown after the immersion tests of nanocomposite (with SWNTs and SWNTs-COOH). It is possible to observe the different colour of the solution. The PLGA-SWNT medium (Fig. 9b) remained essentially clear, whereas in the case of the carboxylate tubes, the degrading medium changed colour from grey to black during degradation, indicating the transfer of nanotubes from the sample to the incubation medium (Fig. 9a). In agreement with these visual observations, Fig. 9 shows the results of UV-VIS spectroscopy applied to the incubation medium for the SWNTs-COOH nanocomposites, for different degradation times. The absorbance of the medium clearly increases during incubation time confirming the dispersion of CNTs on the medium.

In fact, the presence of carboxylic groups in functionalized SWNTs-COOH accelerated the hydrolytic degradation of the PLGA matrix and the weight loss of the nanocomposites. The degradation process of the polymeric matrix involved cross-linking/chain-scission mismatch, the second mechanism clearly dominated in PLGA/SWNTs-COOH systems.

This behaviour suggests the selective interaction of water at the interface between the nanotubes and the polymeric matrix, similar to the behaviour reported at the fiber-matrix interface in conventional composites [35, 36]. It is well know that this interaction is mainly controlled by the fiber treatment, functionalization and coatings of fibers. Although it can be assumed from FT-IR, DSC and TGA results that the SWNTs-COOH are not covalently linked to the PLGA copolymer, the interaction of the functionalized

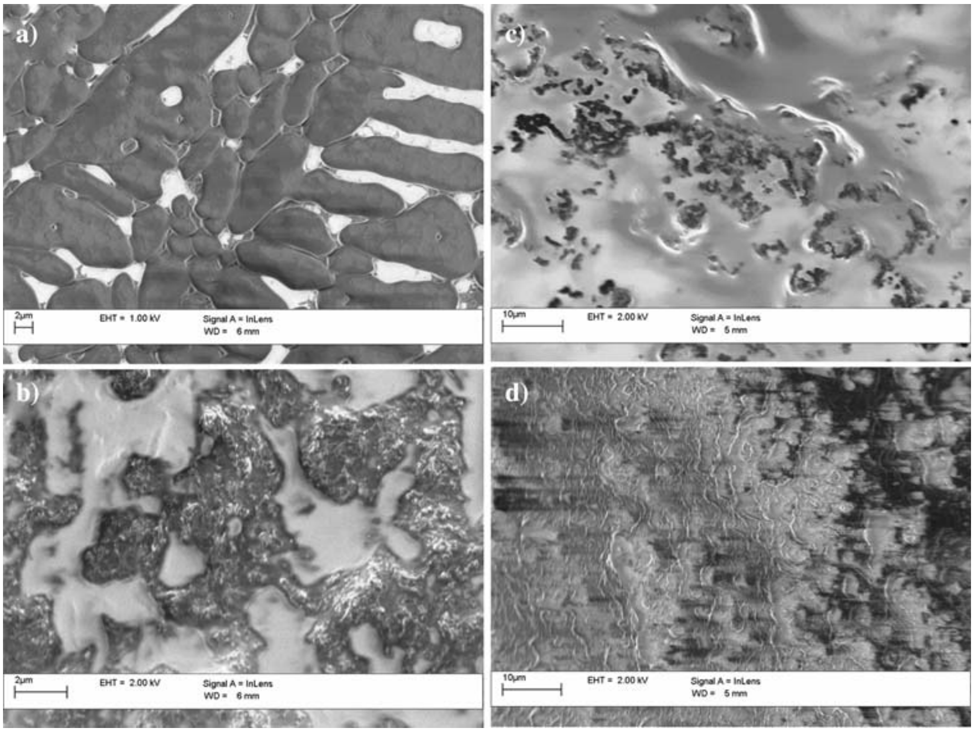

Fig. 8 SEM pictures of PLGA/SWNTs surface after 4 weeks of degradation (**a**) and after 9 weeks of degradation (**b**). Comparative SEM pictures of PLGA/SWNTs (**c**) and PLGA/SWNTs-COOH (**d**) surface after 9 weeks of degradation

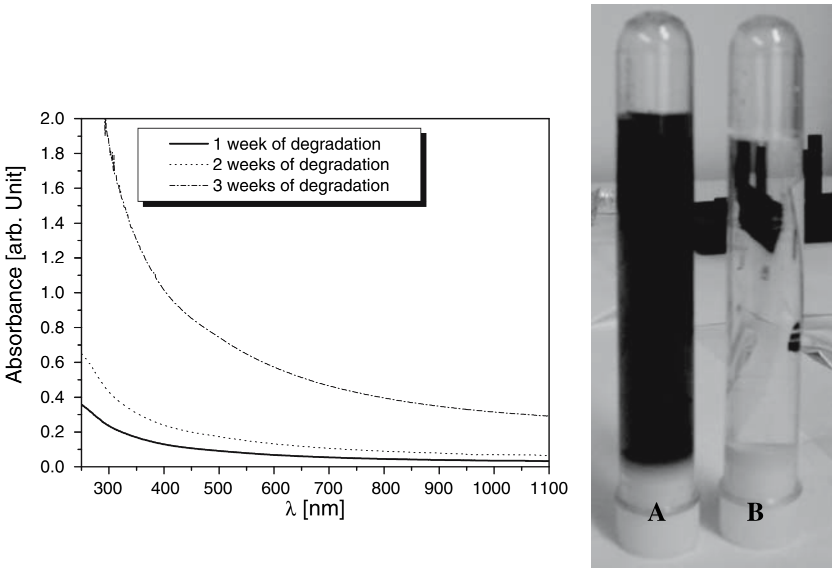

Fig. 9 UV-VIS spectra of hydrolitic medium for different incubation times. Images of hydrolytic medium for nanocomposite based on SWNTs (A) and SWNT-COOH (B)

carboxylate nanotubes is high enough to promote a higher hydrolytic degradation with respect to other two systems studied. Moreover, it should also be considered that the higher dispersibility of the functionalized SWNTs-COOH offers a better surface interaction for solvent interaction that in the case of SWNTs that forming bundles offer a lower surface interaction with the polymer.

3.3.5 *pH changes*

In our study, the pH level of the surrounding medium was measured periodically. No significant decrease in the pH was measured when samples of 10 mg were immersed in a volume of 20 ml solution. It is evident that very low ratio of sample weight to solution volume allows to a higher degree of dilution of the extracted material. When higher mass samples (500 mg) were used with the same volume of solution, the pH of the fluid was lowered in agreement with the expected water-soluble oligomers with carboxylic groups produced by the hydrolytic degradation of the PLGA [37]. The pH of the medium was 4.0 for PLGA/SWNT while it was 6.0 in the case of PLGA/SWNT-COOH after 9 weeks of degradation. This pH variation gives a further confirmation of what stated above about the carboxylate nanotube and polymer matrix interaction, and their effects on the kinetics of degradation.

3.3.6 *Thermal degradation*

The effects of the hydrolytic degradation on the TGA results were obtained for the three materials tested: PLGA, PLGA/SWNTs and PLGA/SWNT-COOH are reported in Fig. 10. The thermal degradation of the pristine PLGA produces a single peak at about 365 °C. The effects of carbon nanotubes on the thermal degradation behaviour of the nanocomposites before hydrolysis are not evident as the peak associated to the degradation of the polymer matrix are almost identical in all samples (the thermal degradation of the nanotubes cannot be observed at the lower percentage used). However, a different degradative profile was observed for samples degraded in-vitro for 9 weeks. The shift to lower temperatures (ca. 90 °C) of the peak associated to the degradation of the matrix is clearly associated to the reduction of the molecular weight of the matrix as a consequence of the hydrolytic behaviour after exposure to simulated biological fluids. Moreover, carboxylate tubes seem to induce a slightly higher thermal stability to the

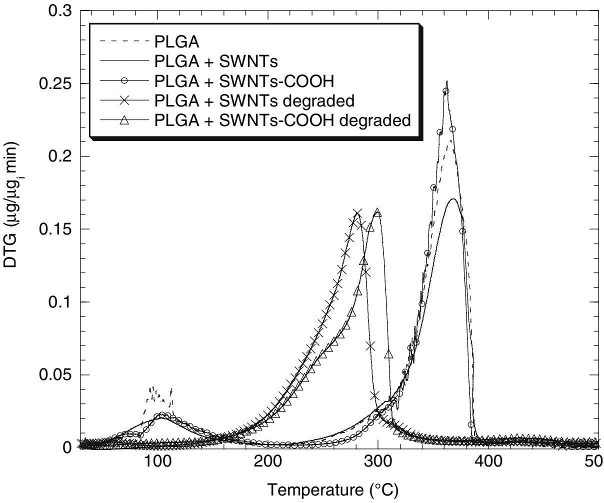

Fig. 10 Derivative oxidation thermograms of degraded PLGA, PLGA/SWNTs and PLGA/SWNTs-COOH samples

nanocomposites while its effects on the hydrolytic degradation were in the opposite direction.

4 Conclusions

Nanocomposites made with biodegradable PLGA matrix and CNTs were processed by solvent casting to produce films that could be potentially used for the production of scaffolds. The main objective was to analyze the effects of the incorporation of nanotubes and of their functionalization on the structural behaviour of the films produced. In particular, the in-vitro degradation kinetics of the composite samples was evaluated by analysing their weight loss, glass transition, infrared spectroscopy and morphological changes as a function of the hydrolysis time in normal physiological conditions (pH 7.0 at 37 °C).

An increasing in the mechanical properties was evaluated by dynamical mechanical analysis, the nanocomposite based on carboxylic nanotubes shows the higher storage modulus that indicates that stress transfers from the matrix to the functionalized CNTs.

The incorporation of SWNTs increases the dimensional stability of the polymeric samples but they do not seem to significantly modify the kinetics and the mechanism of the hydrolytic erosion with respect to the neat PLGA. The presence of carboxylic groups in functionalized SWNTs-COOH accelerated the hydrolytic degradation of the PLGA matrix and the weight loss of the nanocomposites. Although the functionalization of carbon nanotubes offers better possibilities for their dispersion in the PLGA matrix, it is also clear that its higher solubility and the promotion of a higher PLGA-water interaction must be considered in the future development and possible standardization of biodegradable biomaterials.

In the rapidly growing field of tissue engineering, novel biomaterials are intensely being examined. These studies suggest that the PLGA properties can be modified introducing a small percentage of CNTs, pristine and carboxylated ones. The degradation kinetics of nanocomposites for scaffolds can be engineered by varying the CNT content and functionalization. The combination of biodegradable polymers and carbon nanotubes (CNTs) opens in fact a new perspective in the self-assembly of nanomaterials and nanodevices for biomedical applications. Future studies will include the mechanical testing of these materials during degradation as well as in-vivo degradation, cell response and toxicity studies.

Acknowledgements This study was carried out with the support of the European Union, within the framework of the NANOBIOCOM FP6-EC project. The authors, I.A. and M.D. acknowledges the financial support from the National Consortium of Materials Science and Technology (INSTM). We acknowledge the help of Dr Federica Meloni for the SEM analysis as well as for technical support. Interesting discussions with Dr Jurado Oñate María Jesús (Inasmet-Spain) were highly appreciated.

References

1. M. S. DRESSELHAUS, G. DRESSEHAUS and P. C. EKLUND, in “Science of fullenrenes and carbon nanotubes” (Academic Press, New York, 1996), Chap. 19
2. R. SAITO, G. DRESSEHAUS and M. S. DRESSELHAUS, in “Physics properties of carbon nanotubes” (World Scientific, New York, 1998)
3. T. W. EBBESEN, *J. Phys. Chem. Solids* **57** (1996) 951
4. C. J. LEE, J. PARK, S.Y. KANG and J. H. LEE, *Chem. Phys. Lett.* **326** (2000) 175
5. L. F. SUN, L. I. U. ZQ, M. A. XC, Z. Y. ZONG, S. B. TANG, Z. T. XIONG, D. S. TANG, W. Y. ZHOU, X. P. ZOU, Y. B. LI, K. L. TAN, S. S. XIE and J. Y. LIN, *Chem. Phys. Lett.* **340** (2001) 222
6. H. DAI, M. SHIM, R. J. CHEN, Y. LI and N. W. S. KAM, *NanoLetters* **2** (2002) 285
7. M. A. CORREA-DUARTE, N. WAGNER, J. ROJAS-CHAPANA, C. MORSCZECK, M. THIE and M. GIERSIG, *NanoLetters* **4** (2004) 2233
8. W. HUANG, S. TAYLOR, K. FU, Y. LIN, D. ZHANG, T. W. HANKS, A. M. RAO, Y. -P. SUN and W. HUANG, *NanoLetters* **4** (2002) 311
9. X. ZHANG, T. LIU, T. V. SREEKUMAR, S. KUMAR, V. C. MOORE, R. H. HAUGE and R. E. SMALLEY, *NanoLetters* **3** (2003) 1285
10. L. VALENTINI, I. ARMENTANO, J. BIAGIOTTI, J. M. KENNY and S. SANTUCCI, *Diamond Relat. Mater.* **12** (2003) 1601
11. G. X. CHEN, H. S. KIM, B. H. PARK and J. S. YOON, *J. Phys. Chem. B* **109** (2005) 22237
12. L. VALENTINI, D. PUGLIA, I. ARMENTANO and J. M. KENNY, *Chem. Phys. Lett.* **403** (2005) 385
13. C. A. DYKE and J. M. TOUR, *J. Phys. Chem. A* **108** (2004) 11152
14. K. BALASUBRAMANIAN and M. BURGHARD, *Small* **1** (2005) 180
15. V. MAQUET, A. R. BOCCACCINI, L. PRAVATA, I. NOTINGHER and R. JEROME, *Biomaterials* **25** (2004) 4185
16. Y. Y. YANG, M. SHI, S. H. GOH, S. M. MOOCHHALA and J. HELLER, *J. Control. Release.* **88** (2003) 201
17. S. C. J. LOO, C. P. OOI and Y. C. F. BOEY, *Polym. Degrad. Stab.* **83** (2004) 259
18. S. HURRELL and R. E. CAMERON, *J. Mater. Sci. Mater. Med.* **12** (2001) 811
19. L. U. LUSA, C. A. GARCIA and A. G. MIKOS, *J. Biomed. Mater. Res.* **46** (1999) 236
20. X. WEN and P. A. TRESCO, *Biomaterials* **27** (2006) 3800
21. K. REZWAN, Q. Z. CHEN, J. J. BLAKERA and A. R. BECCACCINI, *Biomaterials* **27** (2006) 3413
22. L. K. CHIU, W. J. CHIU and Y. L. CHENG, *Int. J. Pharm.* **126** (1995) 169
23. A. S. DUNN, P. G. CAMPBELL and K. G. MARRA, *J. Mater. Sci. Mater. Med.* **12** (2001) 673
24. R. A. BLEY, R. C. NIEDNER, G. S. HERRING, G. C. MOTOC, K. D. LEROY and M. B. POST, *Adv. Mater. Sci.* **5** (2003) 354
25. B. WU, J. ZHANG, Z. WEI, S. CAI and Z. LIU, *J. Phys. Chem. B* **105** (2001) 5075
26. E. P .S. TAN and C. T. LIM, *Composites Sci. Technol.* **66** (2006) 1099
27. J. SIEPMANN, K. ELKHARRAZ, F. SIEPMANN and D. KLOSE, *Biomacromolecules* **6** (2005) 2312

28. A. SANTOVENA, C. ALAVREZ-LORENZO, A. CONCHEIRO, M. LLABRES and J. B. FARINA, *Biomaterials* **25** (2005) 925
29. C. A. AGUILAR, Y. LU, S. MAO and S. CHEN, *Biomaterials* **26** (2005) 7642
30. G. KISTER, G. CASSANAS and M. VERT, *Spectrochim. Acta Part. A* **53** (1997) 1399
31. E. ÇATIKER, M. GÜMÜŞDERELIOĞLU and M. GÜNER, *Polym. Int.* **49** (2000) 728
32. A. L. MERCADO, C. E. ALLMOND, J. G. HOEKSTRA and J. M. FITZ-GERALD, *Appl. Phys. A Mater. Sci. Process.* **81** (2005) 591
33. H. W. KIM, C. W. CHUNG, Y. B. KIM and Y. H. RHEE, *Int. J. Biol. Macromol.* **37** (2005) 221
34. M. H. HUANG, S. LI and M. VERT, *Polymer* **45** (2004) 8675
35. X. BIAN, L. AMBROSIO, J. M. KENNY, L. NICOLAIS, E. OCCHIELLO, M. MORRA, F. GARBASSI and A. DI BENEDETTO, *J. Adhesion. Sci. Technol.* **5** (1991) 377
36. X. BIAN, L. AMBROSIO, J. M. KENNY, L. NICOLAIS and A. DI BENEDETTO, *Polym. Com.* **12** (1991) 333
37. A. GOPFERICH, *Biomaterials* **17** (1996) 103